A Study of Substrate Effects in Indentation Hardness Tests of Thin Films by Use of Indentation Hysteresis

Roger Y. Lo and David B. Bogy
Computer Mechanics Laboratory
Department of Mechanical Engineering
University of California, Berkeley
Berkeley, CA 94720

ABSTRACT

Repeated indentations at the same locations on the surface of most materials will generate hysteresis loops. Two types of hysteresis can be identified by detailed examination of the loops. For most materials, indentation hysteresis loops result from the yielding in tension in the unloading processes and re-yielding in the subsequent loading processes. This type of indentation hysteresis can be suppressed (or subjected to shakedown) after a few loading cycles. The processes after shakedown are completely reversible and thus, elastic. The second type of hysteresis can only be found in semiconductors such as silicon, and it is due to a reversible phase transformation that occurs upon the application of sufficient load. The shape of this type of hysteresis curve is quite different from that of the first type. No sign of re-yielding can be observed, and this type of hysteresis is not subject to shakedown. Substrate effects were studied on samples that show shakedownable film hysteresis and non-shakedownable substrate hysteresis. Three diamond indenters with different radii were used. The results showed that the pure film properties can be obtained if the indentation residual depths are kept below 20% of the film thickness.

1 INTRODUCTION

Nanoindentation tests have been widely adopted to study the mechanical properties, such as hardness and elastic modulus, of thin film materials. The unloading process of an indentation test is usually assumed to be elastic, and therefore it can be analyzed by the Hertz elastic contact theory or by Sneddon's[1] solution for the elastic field within a homogenous half space indented by a solid of revolution. However, the purely elastic unloading process can only be observed for a few materials such as fused quartz. The unloading process for most materials usually involves a yielding in tension due to the residual stresses generated in the loading process. If the material is loaded again at the same location with the same maximum force, the second loading process usually contains re-yielding at forces close to the maximum. Again, the second unloading process shows yielding in tension. Therefore, hysteresis loops are generated by the second and subsequent loading cycles. The residual stress generated in each loading process suppresses additional plastic deformation. The hysteresis can be completely suppressed (subjected to shakedown) after a few loading cycles. After shakedown, both the loading and unloading processes are purely elastic.

Indentation hysteresis can also be generated in semiconductor materials such as silicon and germanium. Unlike the hysteresis mentioned above, hysteresis in these materials does not have obvious signs of re-yielding in the reloading process, and thus their deformation mechanisms are different from the one mentioned previously. Silicon experiences phase transformations from the semiconductor state to the denser metal state

under load. This transformation is reversible and not suppressible (or subject to shakedown). This means that hysteresis still exists after many cycles of repeated indentation. Using these two types of indentation hysteresis, we can study the substrate effects on the nanoindentation techniques of film/substrate systems. We are particularly interested in the films a few nanometers thick used in the magnetic recording slider-disk interface.

Thin film materials have been used as protective layers for the disks and sliders in hard disk drives for several years. As the demand for higher storage capacity increases, the gaps between read-write heads and the magnetic data layers on the disks have become smaller. Thus, the flying heights of the sliders and the thicknesses of the protective thin films have been greatly reduced. As the films become thinner, substrate effects — influences from substrates on the measurements of film properties — are inevitable in attempts to characterize them by nanoindentation techniques. Therefore, it is important to understand the influences of substrates in nanoindentation tests. Substrate effects can be studied on the samples with shakedownable film hysteresis and non-shakedownable substrate hysteresis (or vice versa) with a few cycles of repeated loadings that are enough to shakedown the film hysteresis. Substrate effects can also be quantified by the remaining hysteresis energy. In this study, a 100 nm permalloy film deposited on silicon was examined in this way.

A Hysitron tester was used to make indentation tests. Like the Atomic Force Microscope (AFM), the Hysitron tester can provide topography mapping of specimens by tracing the

surface contours of the sample with micro-Newton loads. However, unlike the conventional AFM, this device can also be a force-generating and depth-sensing instrument capable of providing load-displacement curves at user-specified locations and forces. The resolutions of the system are about 0.2 μN in force and 1 nm in depth. Though the load is significantly greater than the 1-10nN loads of the conventional AFM, the lateral resolution is the same and is determined by the tip radius. The indenters used in this study are made from diamond and have the shape of a triangle-based, cube corner, pyramid. Their tip radii are 50 nm, 160 nm, and 334 nm for tip 18, tip 47, and tip 20, respectively.

2 HYSTERESIS GENERATED BY INDENTATION CYCLES OF LOADING AND UNLOADING

A single load-unload cycle is usually used in indentation tests. Figures 1(a) and 1(b) show two often-used single-cycle loading functions versus loading time. The extra segment in Fig 1(b), which holds the indenter at maximum load for few seconds, is used for materials with creep characteristics. Analyses based on Sneddon's[1] solution or Hertz contact theory are usually applied to the unloading part of the cycle, since the unloading process is assumed to be purely elastic. This means that if a second loading cycle were generated at the same location immediately after the first cycle, the second loading process would follow the first unloading curve, and so would the second unloading curve. This is true for materials such as fused quartz. Figure 2 shows the load/displacement curve for fused quartz under double-cycle loading of 100 μN. It is obvious that the first unloading curve, the second loading curve, and the second unloading curve overlap one another. Note that the unloading curves are straight lines with a slightly curved portion for loads lower than 20 μN.

However, the purely elastic unloading assumption is not true for most materials. Repeated indentation at the same location usually generates hysteresis loops. Figures 3(a), (b), (c), and (d) show a doubled-cycled loading function and the load/displacement curves of double-cycled loading for steel, nickel phosphorus (NiP) and silicon <100>, respectively. For all of the cases shown, it is clear that the second loading curves do not coincide with the first unloading curves. The second cycles form closed loops. However, the graph shapes of the hysteresis of steel and NiP are very different from that of silicon.

The silicon hysteresis graph is formed by two relatively smooth curves, while the curves of steel and NiP have kinks. This suggests that the deformation mechanism of silicon under repeated indentation is different from that of steel or NiP. Both deformation mechanisms are discussed in detail in the next subsections.

2.1 Hysteresis formed by elastic-plastic deformation

Consider the graphs for steel and NiP in Fig 3(b) and 3(c). There are kinks on the first unloading, the second loading, and the second unloading curves. The kinks on the unloading curves appear at very low loads while the kinks of the second loading curve are close to the maximum load (displacement). The kinks represent a sudden softening mechanism in the materials. Therefore, the kinks are signs of the transition from elastic processes to plastic processes, i.e. the onset of plastic deformation. Moreover, the kinks on the unloading curves represent a yielding in tension while the kink on the reloading curve indicates a yielding in compression. These observations agree with the prediction by Johnson[2] and the finite element simulation of repeated indentation of a half-space by a rigid sphere reported in Kral *et al*[3]. In their analysis, Kral *et al* mentioned that yielding during unloading is caused by a continuous increase in both the tensile hoop and the compressive radial stresses upon the removal of the approximately uniform contact pressure. Thus, the kinks on the unloading curves occur when the loads are vanishing, since larger differences between the tensile hoop stresses and the compressive radial stresses are created. They also indicated that yielding during unloading occurs on the material surface just outside the maximum contact area and is more likely to be neglected

on materials with larger elastic modulii and smaller strain hardening exponents. This also agrees with the experimental findings here, since the modulus of NiP is about 150 GPa and is larger than the fused quartz modulus of 70 GPa. We do not see any kinks from the unloading curves of fused quartz. Kral *et al* also reported that re-yielding in tension occurs during the second loading process. However, they did not mention the timing of this re-yielding.

Figure 4 shows the load/displacement curve for five load-unload cycles of NiP at the same location. The curves are marked according to the order in which they are generated. Again, the second loading cycle generates a hysteresis loop, in which neither the loading nor the unloading curve coincides with those of the first loading cycle. However, the third through fifth loading cycles do not form hysteresis loops. In fact, the loading and unloading curves of the third through fifth cycles essentially overlap the second unloading curve. There are kinks in the loading and unloading curves at relatively low loads. The kinks appearing at high load in the second loading curve do not occur in the third through fifth loading curves. This result implies that the plastic deformation due to compression is suppressed or subjected to shakedown. Johnson[4] indicates that residual stresses introduced in the early loading cycles are “protective in the sense that they make yielding less likely” on the later loading cycles. Thus, after a few cycles of loading, the hysteresis, which is due to re-yielding, should vanish.

Figure 5 shows the load/displacement curve for steel undergoing five cycles of indentation at the same location. These curves are slightly different from those for NiP,

because the hysteresis of steel is not subjected to shakedown within the first three cycles; it takes an additional loading cycle. Based on the finite element analysis by Kral *et al*, the difference in behavior between steel and NiP may be attributed to the larger elastic modulus or the smaller strain hardening exponent of steel.

The observation of plastic deformation contradicts the assumption of the purely elastic unloading processes when applying elastic theories to hardness measurements. However, since the elastic theories are applied at the maximum load point on the first unloading curve and the onset of plastic deformation appears later at a very low load, the elastic theories can still be applied.

2.2 Hysteresis formed by phase transformations

As seen in Fig. 3, the shape of the hysteresis loop for silicon is very different from those for steel and NiP. There is no kink on the second loading curve, and the second unloading curve almost overlaps the first unloading curve. To further confirm the shape of the hysteresis we used different loads to generate indentation hystereses. Figures 6(a) and 6(b) show the load/displacement curve for silicon for two cycles of indentations at 500 μN and 250 μN respectively. Figure 6(c) shows the normalized plot for both indentations. The hysteresis loops are self-similar according to the normalized plot. There is no observable onset of plastic deformation on the loading curves. Furthermore, there is no sign of yielding in tension while withdrawing the indenter. Therefore, the special shapes of the hysteresis loops for silicon are not due to special loads or stresses. Figure 7 shows

the load/displacement curve for silicon under ten cycles of repeated indentations at the same location. Surprisingly, the hysteresis loop generated in each cycle overlaps the others, and the process shows no sign of shakedown. This means that the shape and size of the hysteresis after ten cycles of repeated indentations remains the same as that of the first cycle. This phenomenon suggests that the deformation mechanism of silicon under repeated indentations is different from that of steel and NiP, which involves elastic-plastic deformation as mentioned in the previous subsection.

To further compare the deformation mechanism behind the indentation hysteresis loops of silicon and NiP we performed two-stage loadings on them. Figure 8 shows a two-stage loading function versus time. This function loads the materials with a smaller load (100 μN in this case) for five cycles and then with a larger load (400 μN in this case) for another five cycles at the same location. In the study, the second-stage load is held fixed while the first-stage load varies. The purpose is to investigate the difference in the second-stage hysteresis due to different first-stage loads. Figure 9 shows the responses of NiP due to two two-stage loading functions. In this experiment the first-stage loads are 100 μN and 200 μN, whereas the second-stage loads are fixed at 400 μN. It is clear that hysteresis loops were generated in the first and second-stages for both loading functions. However, the sizes of the second stage hystereses are significantly different for the different first-stage loads. The second hysteresis associated with the larger first-stage load is smaller than that of the smaller first-stage load. A reasonable explanation of this phenomenon is that more material was deformed and shaken down in the first load stage for larger first-stage loads. Since plastic deformation is not a reversible process, the

material left for plastic deformation for the second-stage load is less for larger first-stage loads. Therefore, the second-stage hysteresis loops are smaller for larger first loads. Note that both of the hystereses exhibited shakedown after tens of cycles of repeated indentations. Figure 10 shows the responses of silicon due to three two-stage loading functions with first-stage loads of 100 μN, 200 μN, and 300 μN, and with second-stage loads fixed at 400 μN. Hystereses are generated in all of the cases in the first and second loading stages. However, unlike the situation for NiP, the sizes and shapes of the second-stage hystereses were not affected by the magnitudes of the first-stage loads. This interesting phenomenon again confirms the view that the deformation mechanism of silicon is reversible and is very different from that of NiP.

Gerk and Tabor[5] reported that silicon and germanium undergo pressure-induced phase transitions from their semiconductor structures to metals. They reported that the transition hydrostatic pressures of silicon and germanium are 19 GPa and 12 Gpa, respectively, which are about 50% greater than the reported hardnesses (12 GPa for Si and 8 GPa for Ga). Clarke *et al*[6] studied the transition of silicon and germanium by measuring their electrical conductivity changes under Vickers and Knoop indentations. They found that the materials become electrically conducting instantaneously as the load is applied. They also reported that "the process is reversible on subsequent unloading and reloading". Hu et al[7] reported that the volume change associated with the transformation process is 21%. Pharr *et al*[8] studied repeated indentations on fused quartz and silicon. They made four cycles of indentations with loads between 0.5 mN and 120 mN in each test. They reported a purely elastic unloading process for fused quartz, but concluded incorrectly

that “it is typical of most metals, ceramics, and glasses”, which is contrary to our findings. Hysteresis generated on silicon was reported and attributed to “one intriguing mechanism …which is a sluggish, but reversible, pressure-induced phase transformation beneath the indenter”. From their cross-section study of silicon <100> under indentation, Wu *et al*[9] also observed the amorphous phase beneath the indenter. Figure 11 shows the phase diagram for silicon[10]. According to the diagram, the pressure required for silicon to transform from a face-centered cubic structure to a centered tetragonal structure is 12 GPa at room temperature (300 K). The stresses generated under the indenter can be roughly estimated as the load divided by the square of the tip radii. For the case of tip 18, which has a tip radius of 50 nm, 25 μN generates 100 GPa. This stress is more than sufficient to induce phase transformation.

Repeated indentation tests were performed on amorphous silicon (a-Si) to further verify the above observations. Figure 12 shows the load/displacement curve for a-Si under five cycles of repeated indentation. It is obvious that the amount of hysteresis of a-Si is significantly smaller than that of crystalline silicon. Like those of NiP and steel, the hysteresis exhibits shakedown after five loading cycles, although the kink of re-yielding on the second loading curve is not easily observable. This test suggests that amorphous silicon undergoes elastic-plastic deformation, rather than phase transition, under the application of repeated indentations. Since application of pressure generates a phase transformation from less dense states to denser states, and since amorphous silicon is the densest state of silicon, it is understandable that hysteresis due to phase transformation cannot be observed.

Since the hysteresis found in silicon and germanium is due to the pressure-induced phase transformation, it is not possible to either subject the hysteresis to shakedown or to find an unloading process that is elastic or whose top portion is elastic. The true hardnesses and modulii of these materials cannot be assessed by the elastic theories. However, the approximate values can still be estimated with the available elastic theories.

3 SUBSTRATE EFFECTS IN THIN FILM MATERIALS

Substrate effects in characterizing the mechanical properties of thin films have been investigated for many years. As the demand for thinner protective films increases in order to decrease the gaps between the sliders and disks in hard disk drives, characterizing the true mechanical properties of the films becomes an even more difficult challenge. The films applied on the current hard disks are about 10 nm thick, associated with an areal density of 3-5 Gb/in^2. To achieve the future areal density goal, which is larger than 100 Gb/in^2, the film thickness will need to be reduced to 3 nm or less. It is unlikely that we can avoid the influence of substrates in attempts to obtain the film properties by means of indentation tests for films with such thicknesses. It is widely believed that as the indention depth decreases the substrate effects will become smaller. However, a limit of this concept certainly exists as the film thickness approaches zero. The rule of thumb is that if the residual depths of indentations do not exceed 20% of the film thickness, then the measured properties are expected to be free of substrate effects. Some rules state that the maximum indentation depth should not exceed 20% of the film thickness to avoid substrate effects. There is essentially no rule that is universally agreed upon. However, all of these rules depend only on the percentage of film thickness that the indenter penetrates and thus, are material-independent.

Since there are two types of indentation hysteresis, i.e. shakedownable and non-shakedownable, the substrate effects of thin-film materials can be studied if the film hysteresis is shakedownable and the substrate hysteresis is not (or vice versa). Tests can

be conducted with various loading forces for five to ten cycles of repeated indentations to shakedown the hysteresis of the film. The remaining hysteresis is due only to the substrate. The substrate effects can be quantified by the hysteresis energy (The area enclosed by the loading and unloading curve) remaining after the loading cycles. A remaining hysteresis energy of zero means there was no influence by the substrate on the indentation processes. Therefore, true film properties can be obtained for an indentation exhibiting zero remaining hysteresis energy.

In our study a 100 nm permalloy (NiFe) film deposited on a silicon wafer (si <100>) was investigated. The permalloy layer consisted of 80% nickel (Ni) and 20% iron (Fe). Three cube-corner tips (90° apex angle), tip18, tip47, and tip20 with radii of 50, 160, and 334 nm, respectively, were used to generate indentation hysteresis curves. The tip radii were calculated by the method proposed by Lo and Bogy[11]. Indentation forces were adjusted to keep the maximum depths between 3 and 120 nm to obtain a complete understanding across the entire film thickness. Since the tip radii are different for the different tips, the indentation forces needed to generate the same depths are expected to be different.

Figure 13 shows a typical load/unload curve and the final hysteresis loop of the permalloy/silicon system after five loading cycles with tip 18 (50 nm radius). The maximum depth and residual depth are 30 nm and 15 nm, respectively. It is obvious that the size of the hysteresis loop decreases with an increase in the number of loading cycles, and becomes saturated in the third cycle. The remaining hysteresis is contributed by the silicon substrate. Figure 14 shows the hysteresis energy versus maximum indentation

forces for all three tips. The hysteresis energies were calculated by integrating the final hysteresis loops over the enclosed areas. As expected, the maximum force required to generate the same amount of hysteresis energy is smaller for a sharper tip. Moreover, the critical forces, i.e. the largest forces allowed to generate zero hysteresis energy, for tip18, tip47, and tip20 are 40 μN, 150 μN, and 400 μN, respectively. Figure 15 shows the hysteresis energy verse maximum indentation depth for the three tips. The critical maximum depths (i.e. the largest maximum depths with zero hysteresis energy) for the three tips are 25 nm, 27 nm, and 33 nm, in order of tip radius. This indicates that the indenters did not experience the substrate effects if the maximum depths were lower than 25 nm, and 27 nm or 33 nm, depending on the tip radius. Figure 16 shows the hysteresis energies versus the residual depths for all three tips. In contrast to the indentation forces and maximum depths, the critical residual depths—which are the largest residual depths with zero hysteresis energies—for all of the tips are 19 nm, which is 19% of the film thickness. This indicates that if the residual depths are smaller than 20% of the film thickness, measurements using the nanoindentation techniques will exhibit no substrate effects.

4 SUMMARY AND CONCLUSIONS

Hystereses were generated by repeated indentations at the same location on the surfaces of several materials. Yielding in tension and re-yielding were observed in metals such as NiP and steel. This type of hysteresis exhibits shakedown after a few cycles of repeated

loading and unloading. The loading processes after shakedown are purely elastic. Phase transformation occurred with repeated indentations on semiconductors such as silicon. Silicon transforms from its semiconductor state to a denser metal state. The transformation was reversed when the load was withdrawn. Therefore, the transformation is reversible and is not suppressed (or does not exhibit shakedown) after multiple loading cycles.

Substrate effects were studied on a 100 nm permalloy film on a silicon substrate. Three indenters with different radii were used to study the influence of tip radius on substrate effects. The study shows that, for the indentation residual depths smaller than 20% of the film thickness, substrate effects can be ignored. This statement is true for all the tips tested regardless of tip radii.

5 ACKNOWLEDGEMENT

This work was supported by the Computer Mechanics Laboratory at the University of California at Berkeley.

6 REFERENCE:

1. I. N. Sneddon, “The relation between load and penetration in the axisymmetric Boussinesq problem for a punch of arbitrary profile”, *International Journal of Engineering Science*, **No**. 3, **pp**. 47-57 (1965)

2. K. L. Johnson, **Contact Mechanics**, Cambridge University Press, Cambridge, U. K., **pp**.171-184

3. E. R. Kral, K. Komvopoulos, and D. B. Bogy, “Elastic-plastic finite element analysis of repeated indentation of a half-space by a rigid sphere”, *J. Applied Mechanics*, **Vol.** 60, **pp** 829-841(1993)

4. K. L. Johnson, **Contact Mechanics**, Cambridge University Press, Cambridge, U. K., **pp**.286-288

5. A. P. Gerk and D. Tabor, “Indentation hardness and semiconductor-metal transition of germanium and silicon”, *Nature*, **Vol**. 271, **pp**. 772-773(1978)

6. D. R. Clarke, M. C. Kroll, P. D. Kirchner, R. F. Cook, and B. J. Hockey, “Amorphization and conductivity of silicon and germanium induced by indentation”, *Physical Review Letters*, **Vol**. 60, **No**. 21, **pp**. 2156-2159 (1988)

7. J. Z. Hu, L. D. Merkle, C. S. Menoni, and I. L. Spain, “Crystal data for high-pressure phases of silicon”, *Physical Review B*, **Vol**. 34, **No**. 7, **pp**. 4679-4684 (1986)

8. G. M. Pharr, W. C. Oliver, and D. R. Clarke, “Hysteresis and discontinuity in the indentation load-displacement behavior of Silicon”, *Scripts Metallurgica*, **Vol**. 23, **pp**. 1949-1952 (1989)

9. Y. Q. Wu, G. Y. Shi, and Y. B. Xu, “Cross-section observation on the indentation of [001] silicon”, *J. of Materials Research*, **Vol**. 14, **No**. 6, **pp**. 2399-2401 (1999)

10. D. A. Young, **Phase Diagrams of the elements**, University of California Press, Berkeley and Los Angeles, California, **pp** 105, (1991)

11. R. Y. Lo and D. B. Bogy, “Compensating for elastic deformation of the indenter in hardness tests of very hard materials”, *J. of Materials Research*, **Vol**. 14, **No**. 6 **pp**. 2276-2282 (1999)

Figure 1(a): A single-cycle loading function with maximum force of 300 μN.

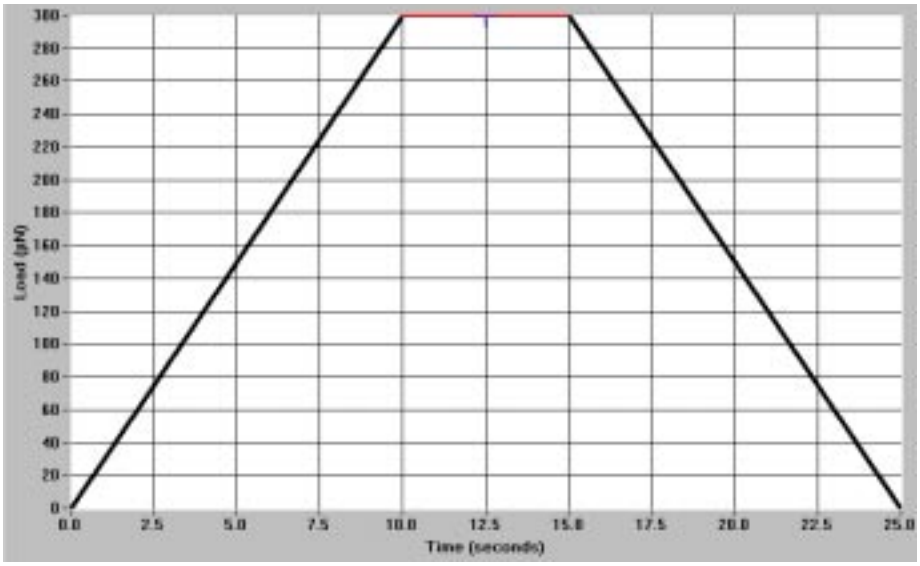

Figure 1(b): A single-cycle loading function with an additional section between loading and unloading.

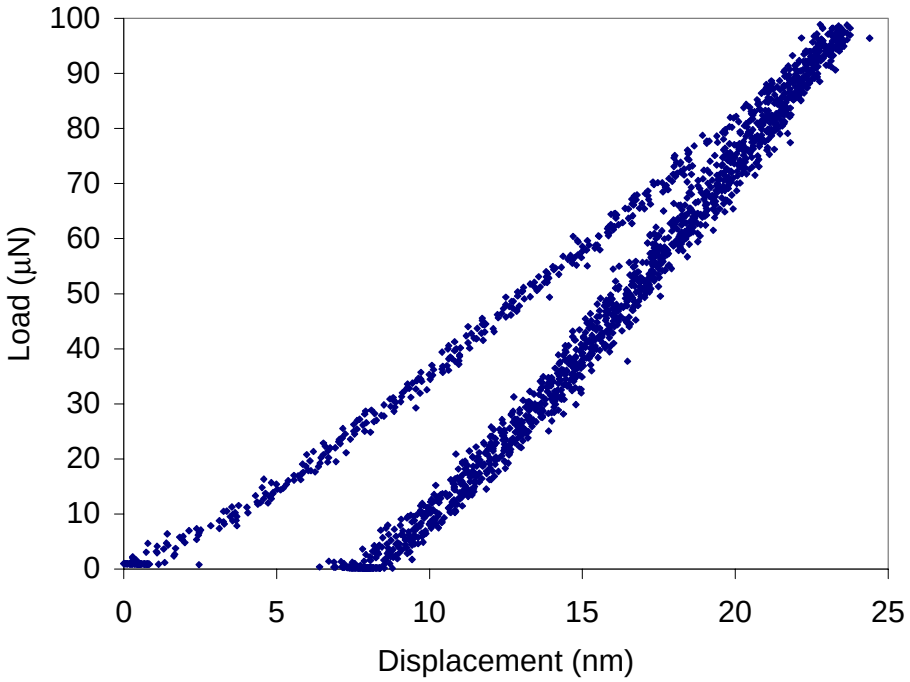

Figure 2: Two cycles of repeated indentations on fused quartz. The loading and unloading curves of the second loading cycle overlap the first unloading curve.

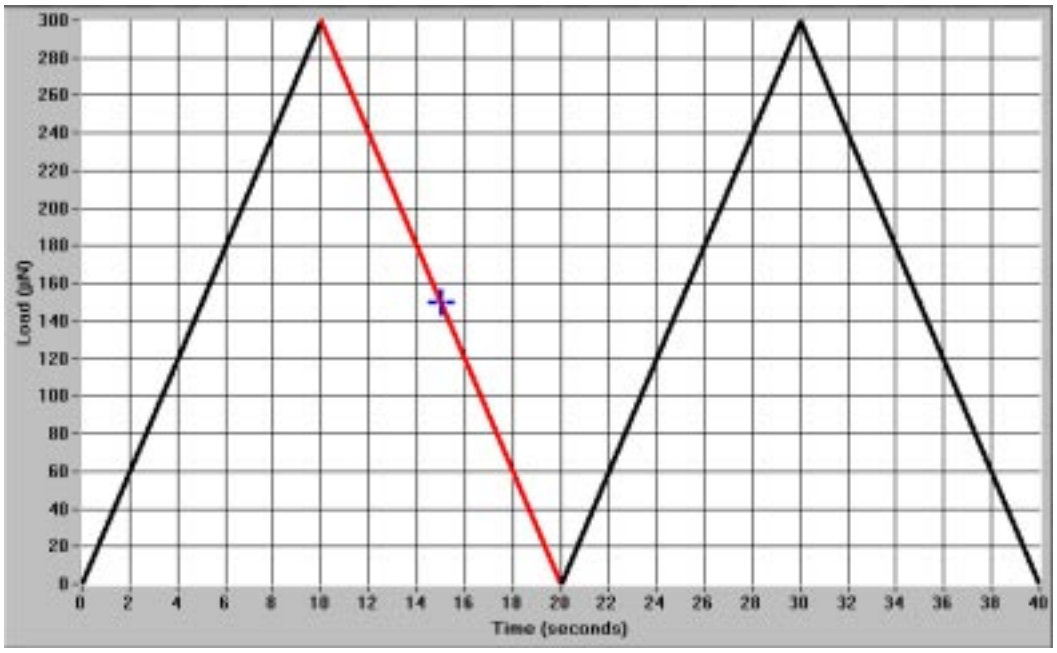

Figure 3(a): A double-cycle loading function with maximum force of 300 μN

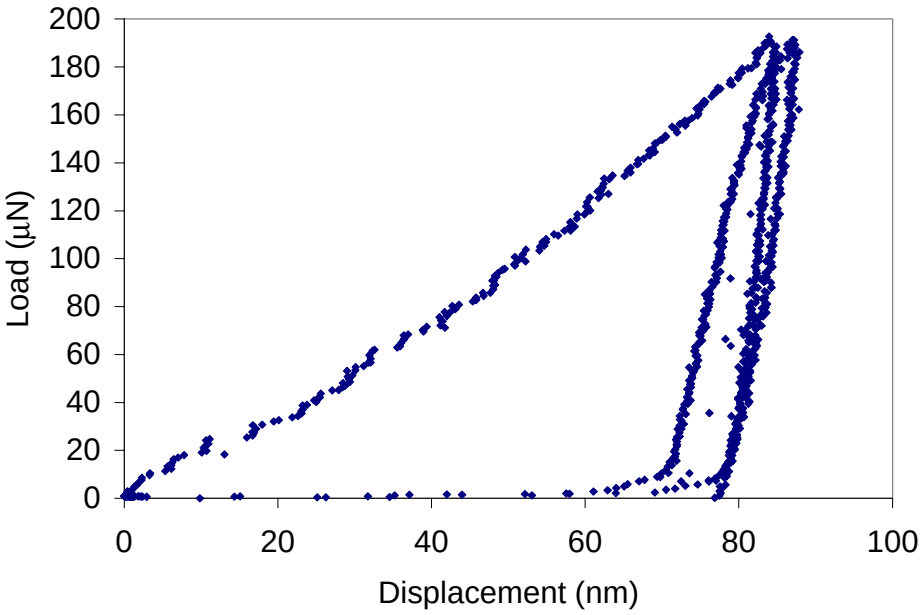

Figure 3(b): The load/displacement curve of steel under a repeated loading for two cycles. Hysteresis is generated by the second cycle.

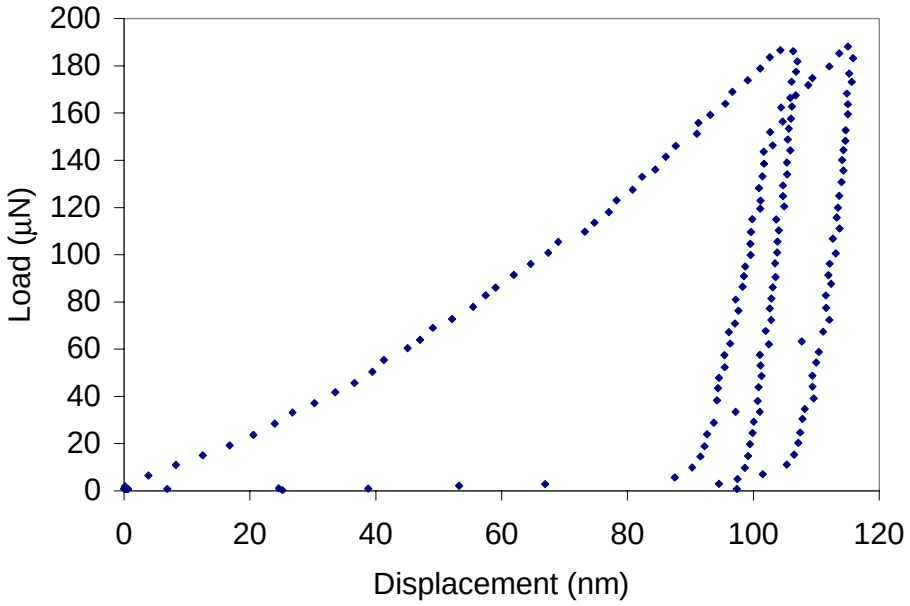

Figure 3(c): The load/displacement curve of Nickle Phosphorus (NiP) under repeated indentations for two cycles. Clear signs of yielding while withdrawing and re-yielding at second loading.

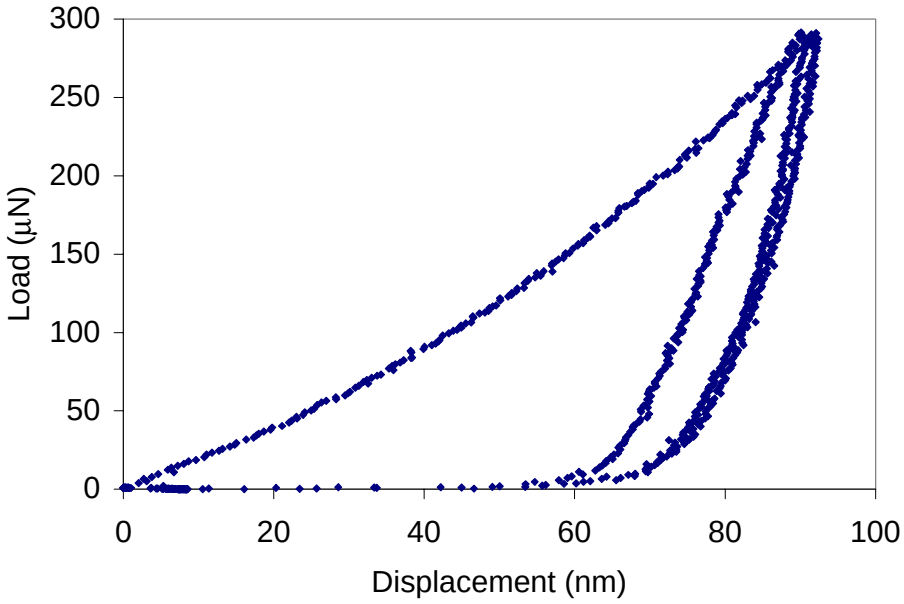

Figure 3(d): The load/displacement curves of silicon <100> under a repeated indentations for two cycles with maximum forces of 300 μN. Hysteresis is generated in the second cycle. However, there is no signs of re-yielding in the curves.

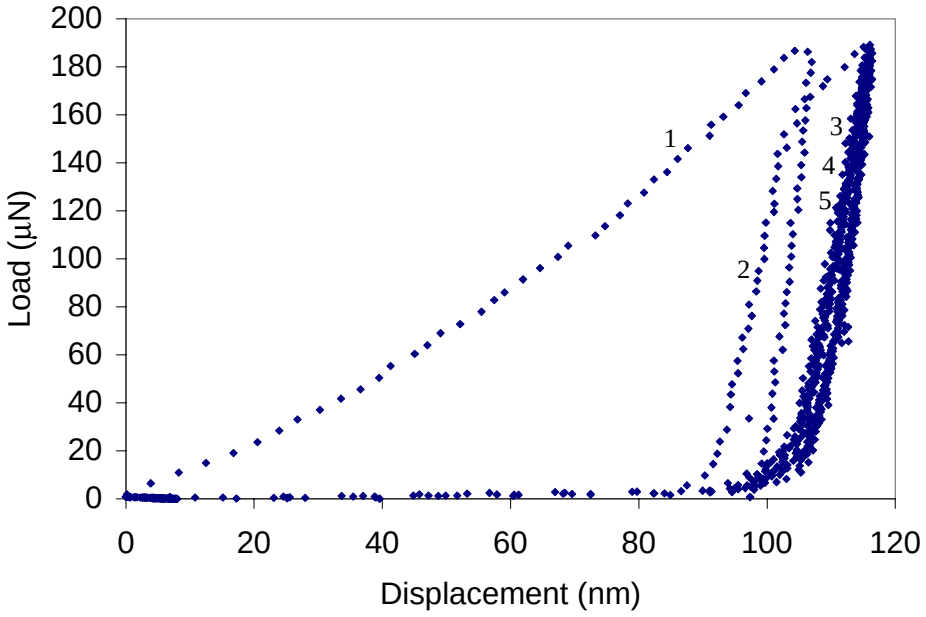

Figure 4: The load/displacement of NiP with five cycles of repeated indentations. The hysteresis generated in the second cycle is subjected to shakedown after the third cycle.

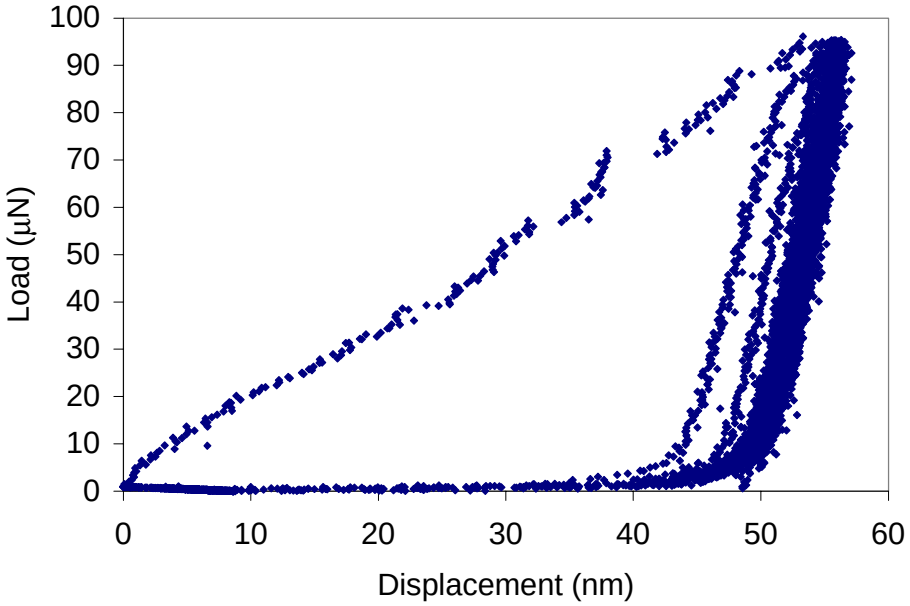

Figure 5: The load/displacement of steel with five cycles of repeated indentations. The hysteresis generated in the second and third cycles are subjected to shakedown after the fourth cycle.

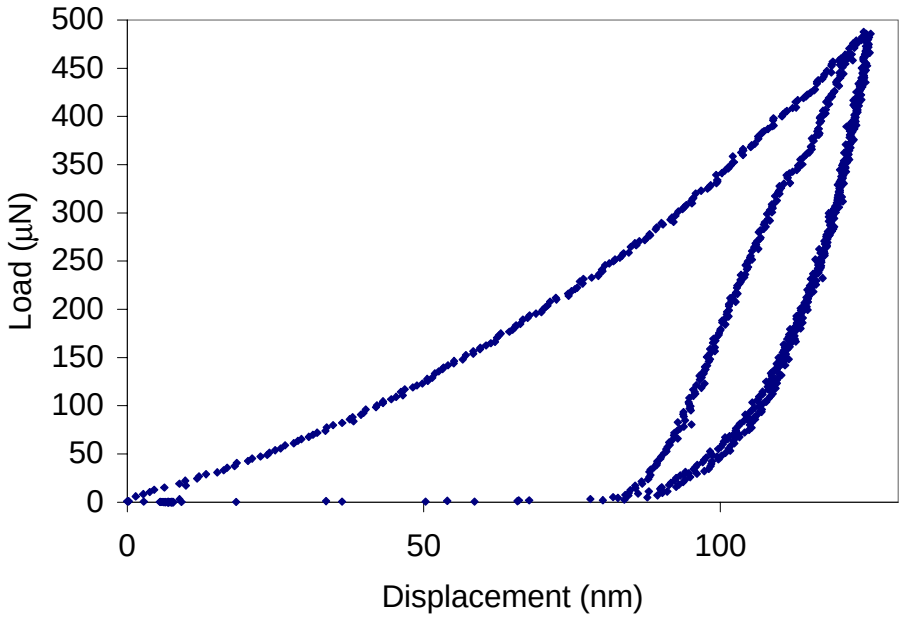

Figure 6(a): the load/displacement curve of silicon <100> under two cycles of repeated indentations with maximum force of 500 μN.

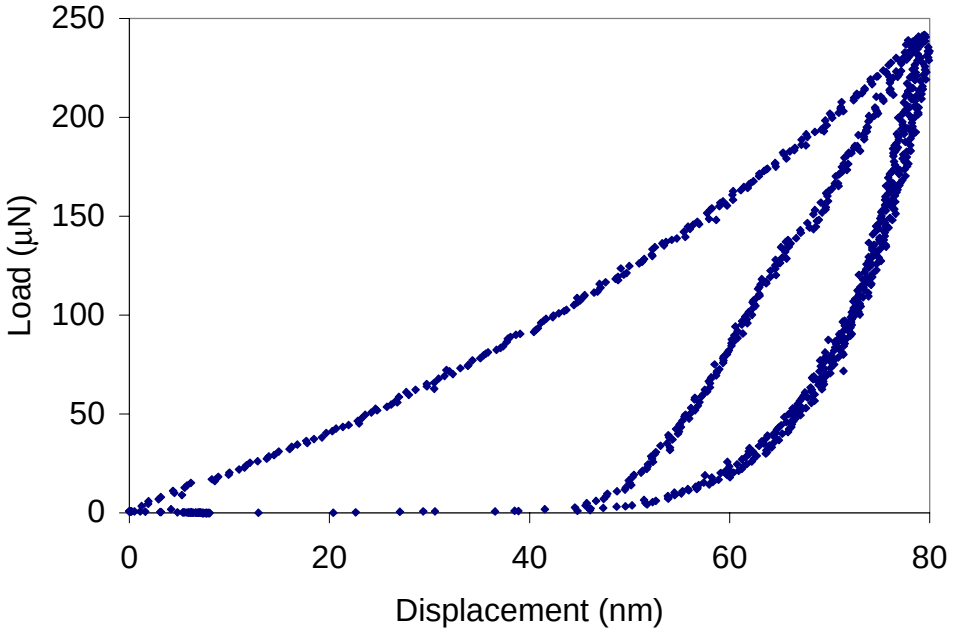

Figure 6(a): the load/displacement curve of silicon <100> under two cycles of repeated indentations with maximum force of 250 μN.

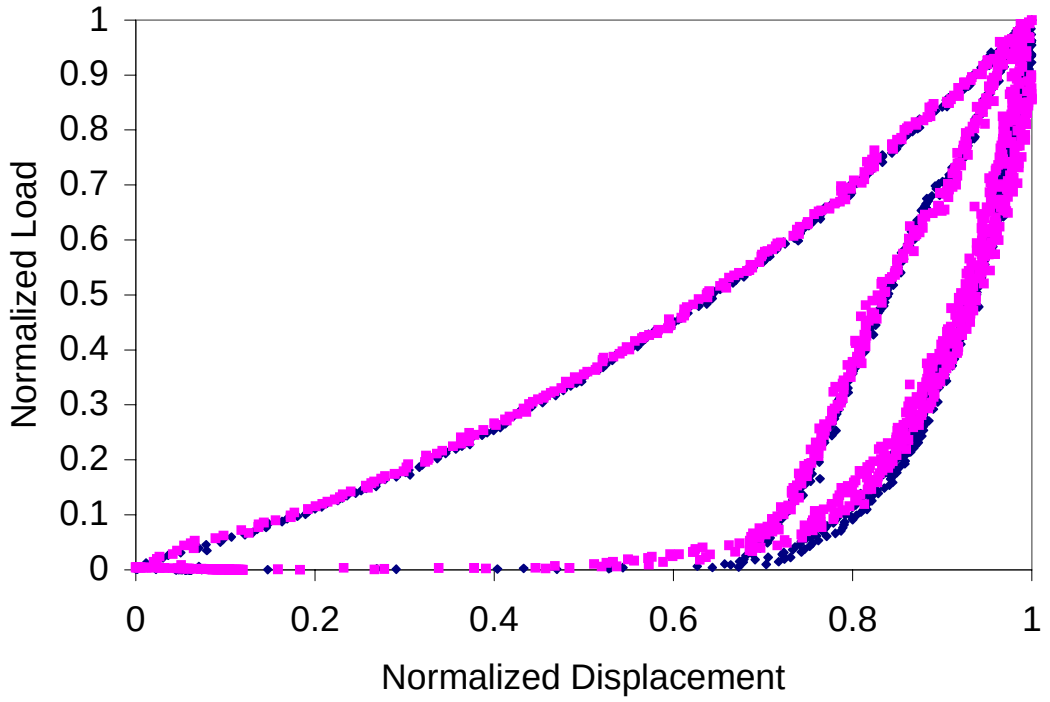

Figure 6(c): The normalized load/displacement curves of Fig. 6(a) and Fig. 6(b). This figure shows that the curves of silicon are self-similar.

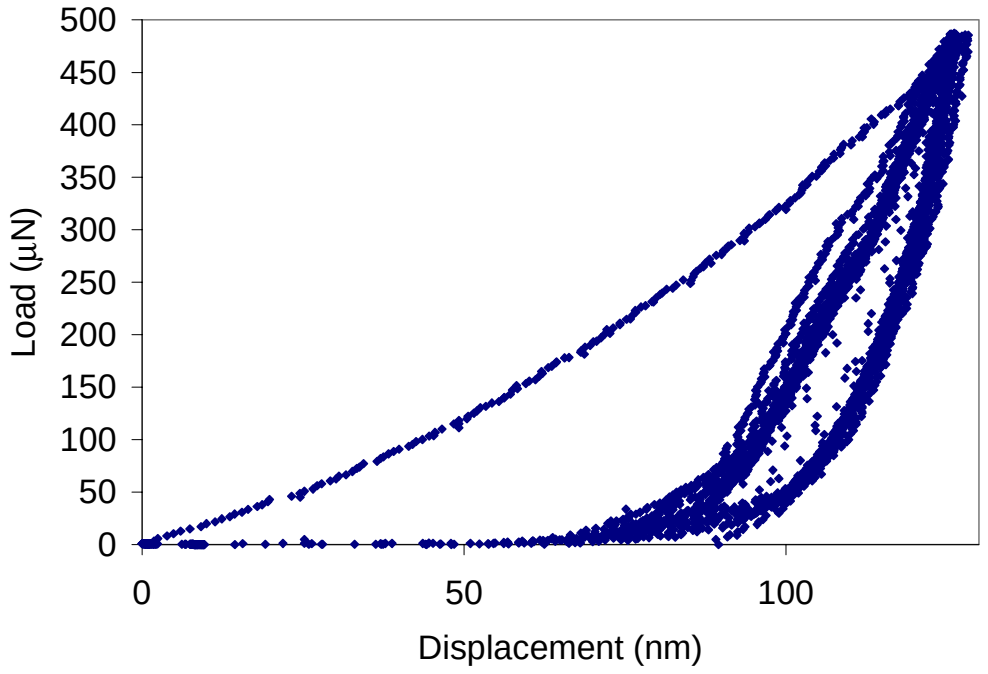

Figure 7: The load/displacement curve of silicon under ten cycles of repeated indentations at the same location.

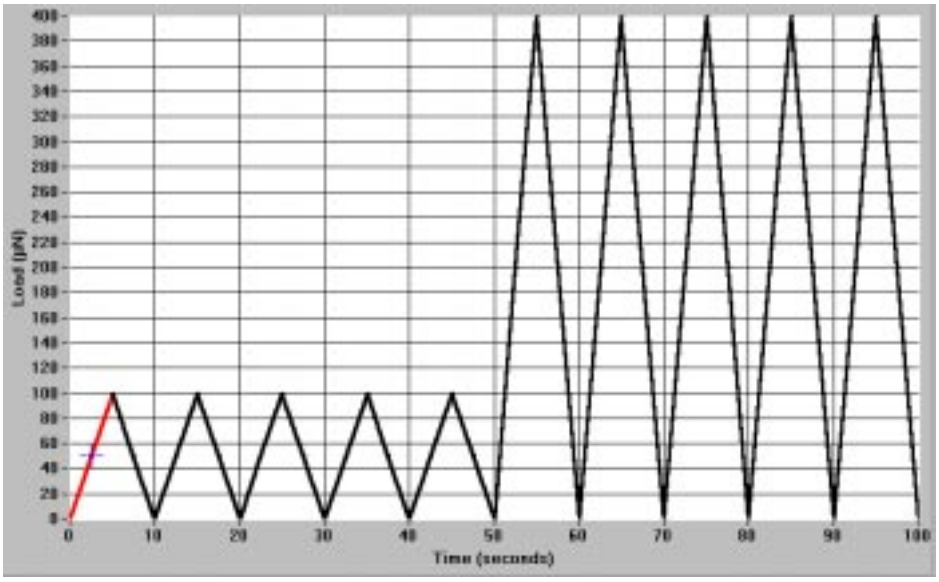

Figure 8: A two-stage loading function

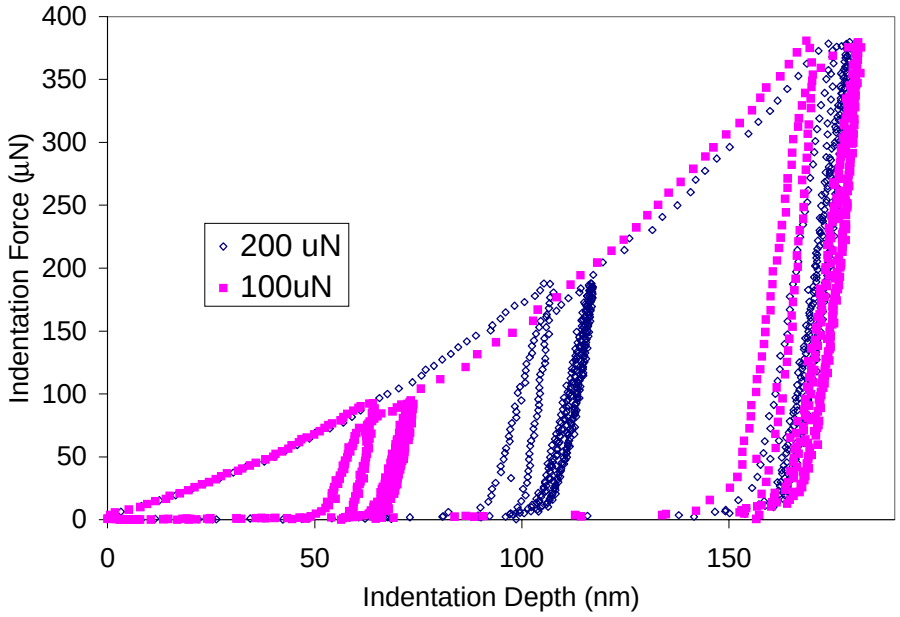

Figure 9: Two-stage loadings on NiP with first loadings of 100 μN and 200 μN. The second loadings remain the same.

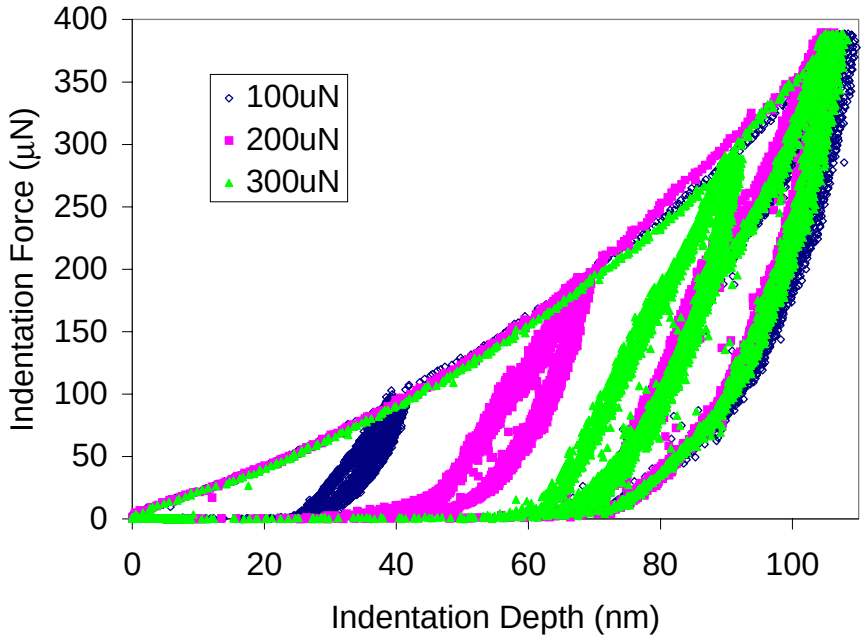

Figure 10: Three two-stage loadings on silicon with first loadings of 100 μN, 200 μN, and 300 μN. The second loadings remain the same.

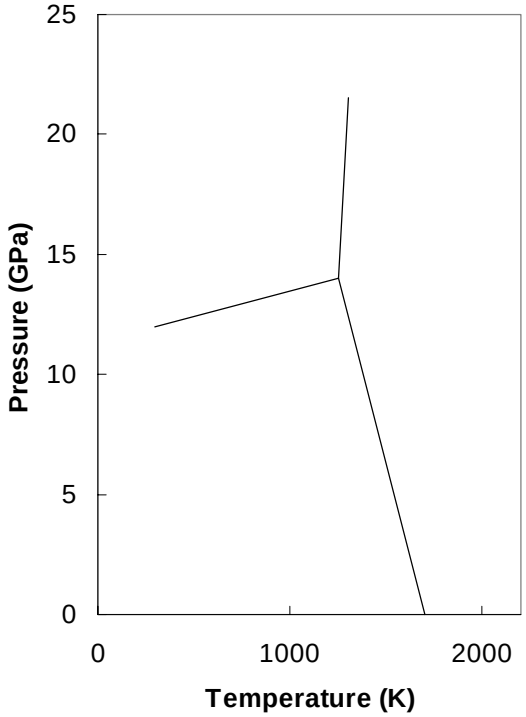

Figure 11: Phase diagram of silicon. The phase transformation pressure at room temperature (300 K) is about 12 GPa. Graph reproduced from Phase Diagrams of the Elements[9]

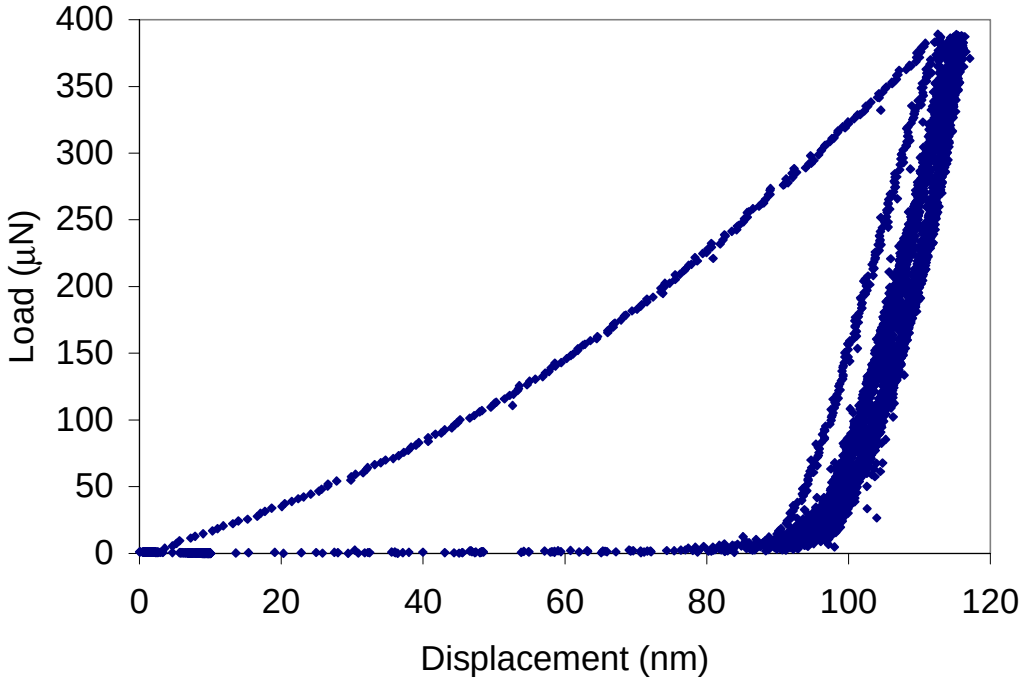

Figure 12: The load/displacement curve of amorphous Si under five cycles of repeated indentations. The hysteresis has been subjected to shakedown shakedowned. Amorphous silicon sample provided by IBM.

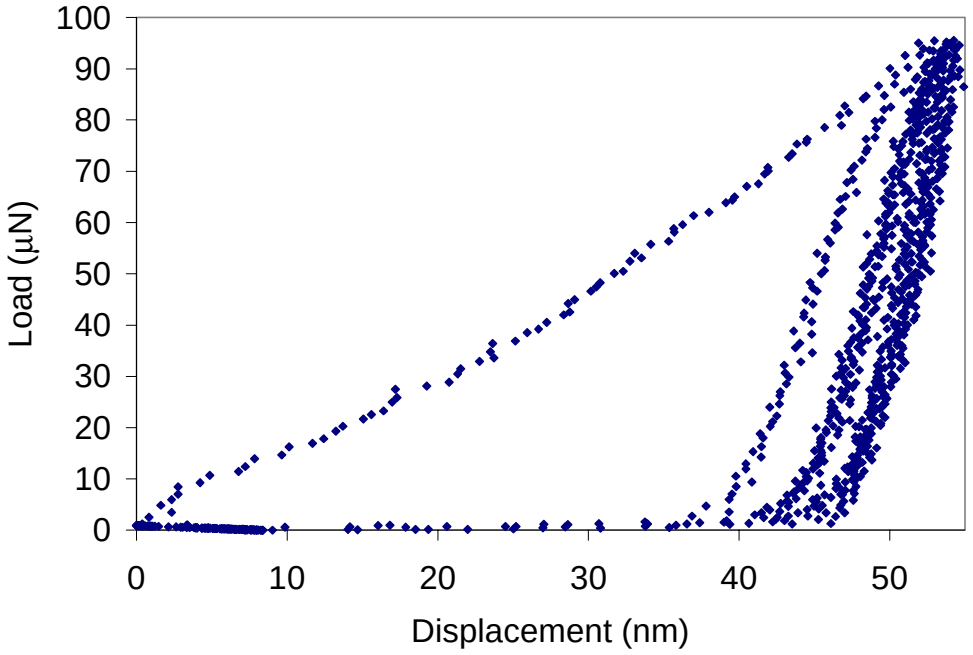

Figure 13: A typical load/unload curve and the final hysteresis loop of the permalloy/silicon system after five loading cycles with tip 18 (50 nm in radius)

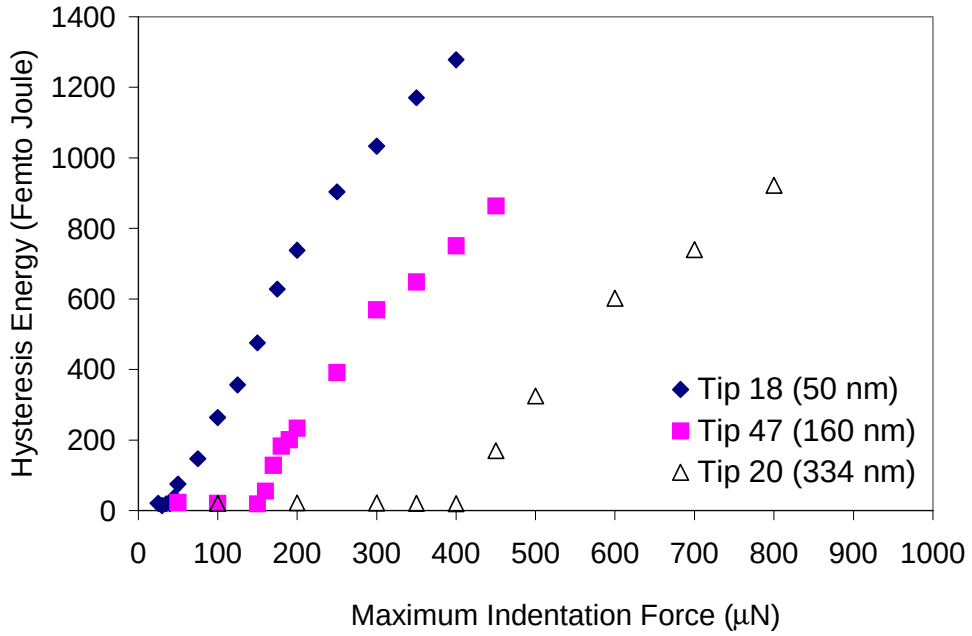

Figure 14: Hysteresis energy versus maximum indentation forces for three tips with variuos tip radii. The hysteresis energies were calculated by integrating the final hysteresis loops over the enclosed areas. The critical maximum indentation forces for the three tips are 40 μN, 150 μN, and 400 μN, respectively.

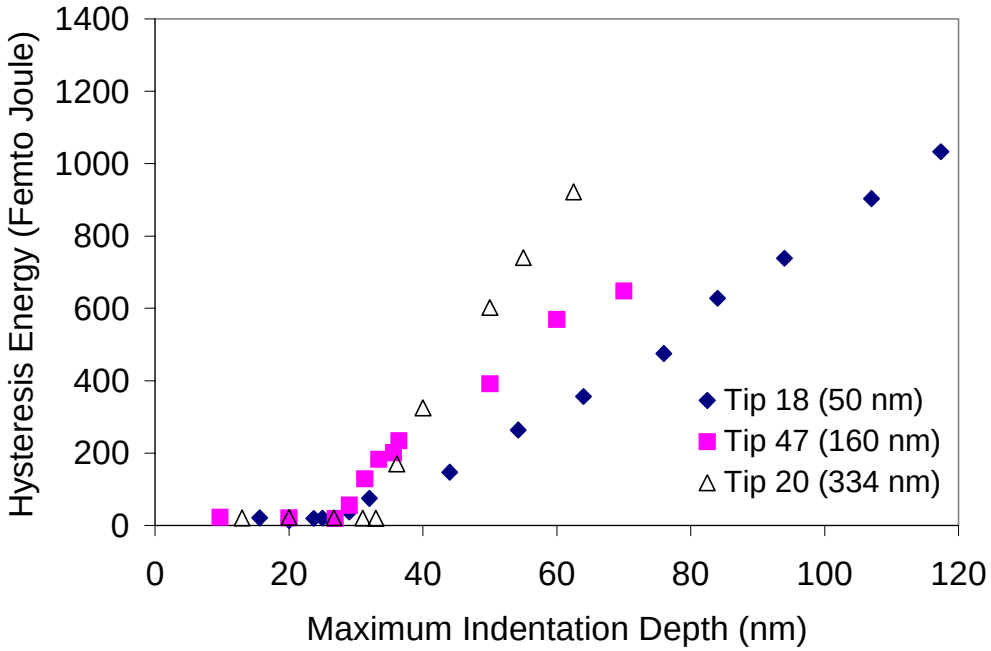

Figure 15: The hysteresis energy versus maximum indentation depths for the three tips. The critical maximum depths for the three tips are 25 nm, 27 nm, and 33 nm, respectively.

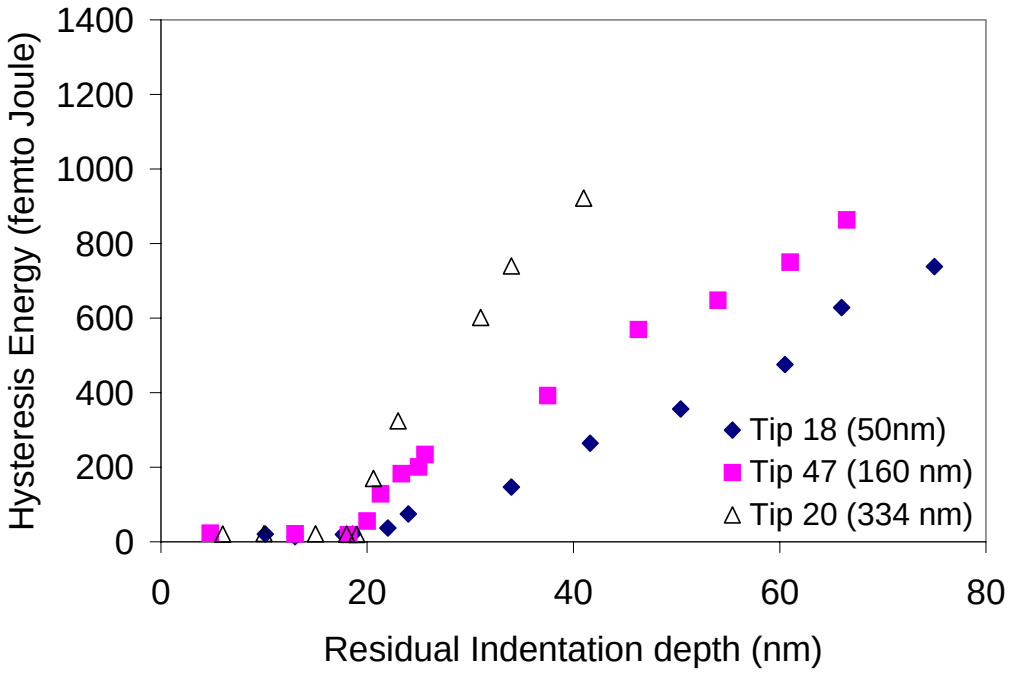

Figure 16: The hysteresis energies versus the residual depths for all three tips. In contract to the maximum indentation forces and maximum depths, the critical residual depths are 19 nm for all of the tips.